Supporting Information for:

Proton-Coupled Electron Transfer Reactions at a Heme-Propionate in an Iron-Protoporphyrin-IX Model Compound

Jeffrey J. Warren and James M. Mayer*
University of Washington, Department of Chemistry Seattle, WA 98195
mayer@chem.washington.edu

Contents:

1. Synthesis of compounds

1.1 Iron(III)protoporphyrin IX monomethyl ester chloride ($Fe^{III}(PPIX_{MME})Cl$)

$Fe^{III}(PPIX_{MME})Cl$ was synthesized by modification of a literature procedure.[1] To a solution of 1.0 g (1.53 mmol) hemin chloride in 250 mL THF and 10 mL CH_3OH were added 0.5 mL concentrated H_2SO_4 over 15 minutes. The reaction progress was monitored periodically by thin layer chromatography (1:1:0.3 hexane:chloroform:CH_3OH) until the concentration of $FePPIX_{MME}$ had reached a maximum (30 hours). The reaction was stopped by the addition of 100 mL EtOAc and 500 mL H_2O. The aqueous layer was extracted 3 times with 100 mL EtOAc and 2 times with 50 mL $CHCl_3$. Each respective extraction was dried over Na_2SO_4, the extracts combined and reduced to dryness under reduced pressure. The resulting purple solid was recrystallized from 4:1 acetone:acetic acid in the presence of NaCl. The resulting purple crystals were filtered, washed with acetic acid, then water and dried under vacuum to give 0.350 g of the desired product (mixture of two isomers, 34 % overall yield). The yield of the corresponding dimethyl ester was 50%. ESI-MS: 630 (M^+). ^1H NMR spectra of high spin ferric protoporphyin IX complexes, like **$Fe^{III}(PPIX_{MME})Cl$**, are typically not very informative because of the very broad peaks.[2] A very common strategy to avoid this complication is addition of CN^- or imidazole to convert the FePPIX-species to the corresponding low spin, 6-coordinate complexes.[3] Thus, purity of **$Fe^{III}(PPIX_{MME})Cl$** was assayed by addition of MeIm to **$Fe^{III}(PPIX_{MME})Cl$** in CD_3CN. The resulting ^1H NMR spectrum (CD_3CN + 5 mM MeIm, 500 MHz) is identical to that of the isolated MeIm complex (below, Figure S1).

1.2 $[Fe^{III}(PPIX_{DME})(MeIm)_2]OTf$

Fe^{III}PPIXCl was fully esterified, using the method described above. The bis(MeIm) triflate salt was also synthesized as described above and in the main text. The ^1H NMR of this complex matches the reported for the corresponding chloride salt.**Error! Bookmark not defined.** ESI-MS: 726 $[M - MeIm]^+$.

(1) Asakura, T.; Lamson, D. W. *Anal. Biochem.***1973**, *53*, 448-451.

(2) Kurland, R. J.; Little, R. G.; Davis, D. G.; Ho, C. *Biochemistry* **1971**, *10*, 2237-2246.

(3) La Mar, G. N.; Satterlee, J. D.; DeRopp, J. S. In *The Porphyrin Handbook*, Vol. 5, Kadish, K. M.; Smith, K. M.; Guilard, R., Eds.; Academic: San Diego, 2000; pp 185-298, esp. pp223-223.

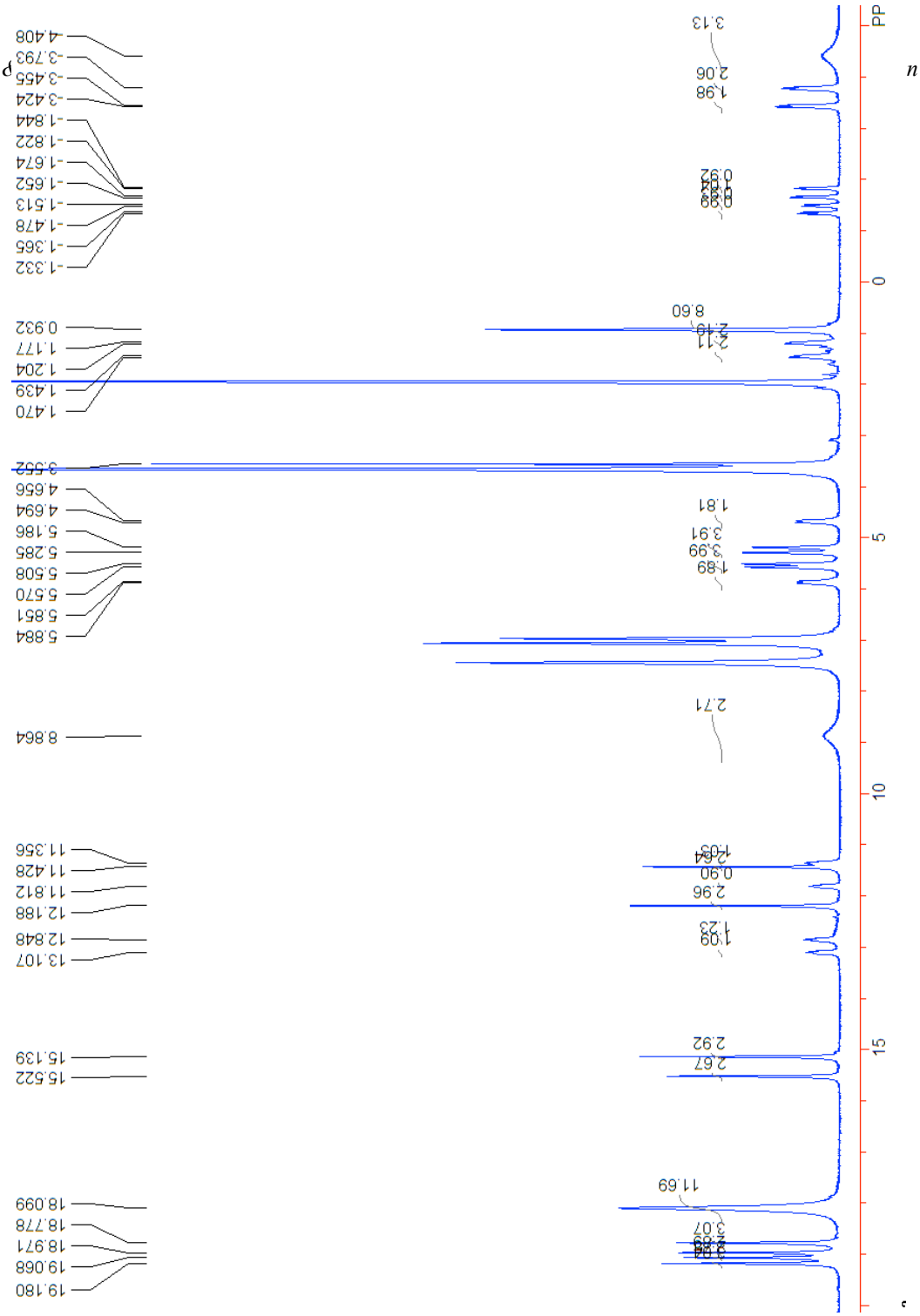

Figure S1. Paramagnetic ^{1}H NMR spectrum of **Fe^{III}~CO_2H** in CD_3CN.

2. Electrochemistry

Electrochemical measurements were performed in a N_2 filled glovebox with approximately 0.1 mM of iron complex and 0.1 M $^{n}Bu_4NPF_6$ in acetonitrile with 5 mM MeIm. The electrodes used were: working electrode, glassy carbon; reference electrode, $Ag^0/AgNO_3$ in electrolyte solution; and auxiliary electrode, platinum wire. All potentials are referenced versus internal ferrocene standard. The estimated errors are ±0.010 V. Scans were taken between 25 and 250 mV s^{-1} in the absence of ferrocene. The midpoint potential of the wave is not dependent upon scan rate. Ferrocene was added and cyclic voltammograms (CVs) were obtained at 25 and 100 mV s^{-1}. Addition of Cp_2Fe resulted in no change in peak potentials for **$Fe^{III/II}$~CO_2H** and **$Fe^{III/II}$~CO_2^-** with respect to CVs run in the absence of Cp_2Fe at a given scan rate. The ratio of peak currents is ~1 at all scan rates. Typical CVs for **$Fe^{III/II}$~CO_2H** and **$Fe^{III/II}$~CO_2^-** are shown in Figure S2.

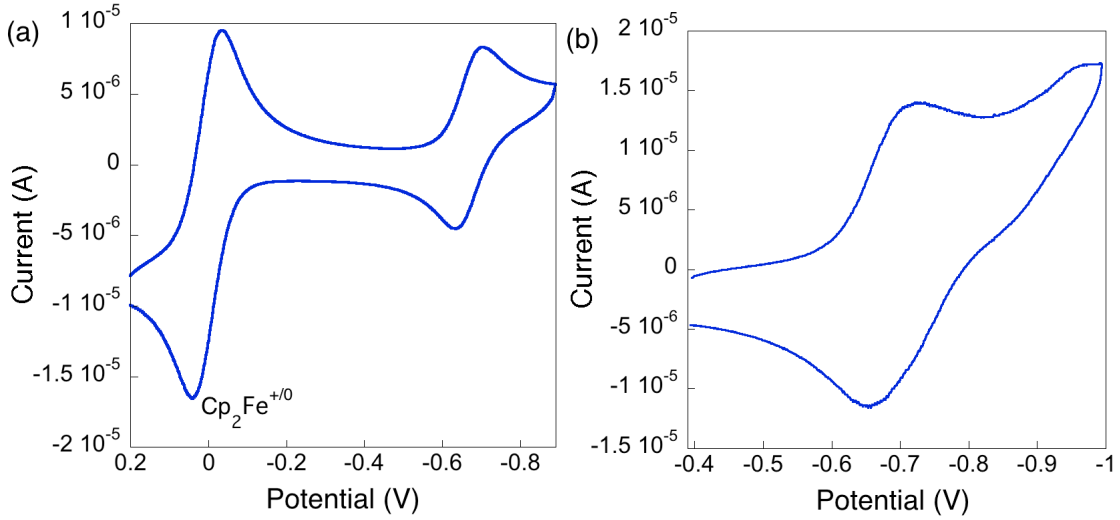

Figure S2. Cyclic voltammograms of (a) **Fe^{III}~CO_2H** and (b) **Fe^{III}~CO_2^-** (from **Fe^{III}~CO_2H** + 1 equiv $^{n}Bu_4NOH$) in MeCN + 0.1 M $^{n}Bu_4NPF_6$ + 5 mM MeIm (potential in V versus $Cp_2Fe^{+/0}$), with scan rate = 100 mV s^{-1}.

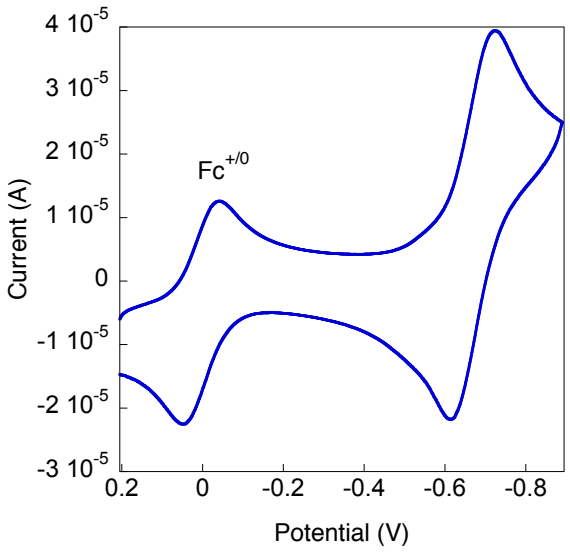

Figure S3. Cyclic voltammograms of $\mathbf{Fe^{III}PPIX_{DME}(MeIm)_2OTf}$ in MeCN + 0.1 M $^{n}Bu_4NPF_6$ + 5 mM MeIm (potential in V versus $Cp_2Fe^{+/0}$), with scan rate = 100 mV s^{-1}.

3. Stopped-flow UV-Vis reactions

3.1 General

All solutions used for kinetics were prepared in a N_2-filled glovebox. The stopped-flow syringes were loaded in the glovebox, and removed in pairs for each respective kinetic run. All measurements were at 298 K. All solutions of $\mathbf{Fe^{III}\sim CO_2^-}$ were freshly prepared from $\mathbf{Fe^{III}\sim CO_2H}$ + 1 equiv DBU immediately prior to use. These solutions were used immediately after mixing because $\mathbf{Fe^{III}\sim CO_2^-}$ has a tendency to precipitate, as described in the main text. Addition of triflic acid (in the presence of 5 mM MeIm) regenerates $\mathbf{Fe^{III}\sim CO_2H}$ indicating that the precipitate compound contains the $FePPIX_{MME}$ macrocycle. Solutions of $\mathbf{Fe^{II}\sim CO_2H}$ were freshly prepared from $\mathbf{Fe^{III}\sim CO_2H}$ + 1 equiv Cp_2Co and were used within 1 hour of preparation. All kinetics were performed in MeCN containing 0.1 $^{n}Bu_4NPF_6$ + 5 mM MeIm. Varying the starting concentration of iron starting material by up to a factor 3 for reactions 1 and 2 (main text) causes no change in the rate constants, indicating that they are first order in iron.

3.2 Determination of pK_a($\mathbf{Fe^{III}\sim CO_2H}$)

The position of equilibrium between $\mathbf{Fe^{III}\sim CO_2H}$ and variable amounts of Et_3N was measured by using the stopped-flow instrument to do a spectrophotometric titration. Reactions are complete in less than 1 second, well before any precipitation can occur. A 2.16×10^{-5} M

solution of **Fe^{III}~CO_2H** was reacted with varying concentrations of Et_3N (pK_a = 18.5[4]) in MeCN/0.1 $^nBu_4NPF_6$/5 mM MeIm. Spectral data were analyzed in SPECFIT using the known spectra of **Fe^{III}~CO_2H** and **Fe^{III}~CO_2^-** as references. The equilibrium constant was obtained by assuming mass balance, an assumption supported by the linearity of the plot in Figure S4.

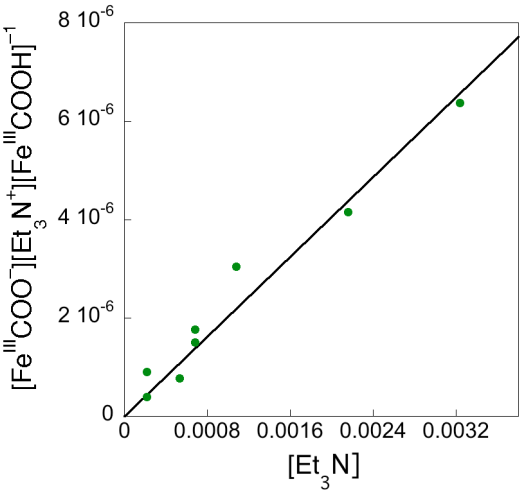

Figure S4. Mass balance plot for the pK_a titration of **Fe^{III}~CO_2H** with Et_3N. The slope gives K_{eq}.

(4) Izutsu, K. *Acid-Base Dissociation Constants in Dipolar Aprotic Solvents*, Chemical Data Series No. 35; Blackwell Scientific: Oxford U.K. 1990.

3.3 Determination of $E(Fe^{III/II}\sim CO_2H)$ and $E(Fe^{III/II}\sim CO_2^-)$ by equilibration with Cp^*_2Fe

The position of equilibrium between $\mathbf{Fe^{III}\sim CO_2H}$ or $\mathbf{Fe^{III}\sim CO_2^-}$ and variable amounts of Cp^*_2Fe (Cp^* = pentamethylcyclopentadienyl anion) was measured by using the stopped-flow instrument to do a spectrophotometric titration, as described above. Reactions are complete in the mixing time of the stopped flow, well before any precipitation of $\mathbf{Fe^{III}\sim CO_2^-}$ can occur (as discussed above). A 9.0×10^{-6} M solution of $\mathbf{Fe^{III}\sim CO_2H}$ was reacted with varying concentrations of Cp^*_2Fe ($E_{1/2}$ = –0.51 V vs. $Cp_2Fe^{+/0}$ in MeCN/0.1M $^nBu_4NPF_6$[5]) in MeCN/0.1 $^nBu_4NPF_6$/5 mM MeIm. Spectral data were analyzed in SPECFIT using the known spectra of $\mathbf{Fe^{III}\sim CO_2H}$, $\mathbf{Fe^{III}\sim CO_2^-}$, $\mathbf{Fe^{III}\sim CO_2H}$, and $\mathbf{Fe^{III}\sim CO_2^-}$ as references. The equilibrium constant was obtained by assuming mass balance, an assumption supported by the linearity of the plots in Figure S5. The reduction potentials $E(\mathbf{Fe^{III/II}\sim CO_2H})$ = 0.655 ± 0.010 and $E(\mathbf{Fe^{III/II}\sim CO_2^-})$ = 0.680 ± 0.010 are in good agreement with the values from cyclic voltammetry (CV). Also, the *difference* in reduction potentials by this method (0.025 ± 0.014 V) is in excellent agreement with the difference in reduction potentials by CV (0.020 ± 0.011 V).

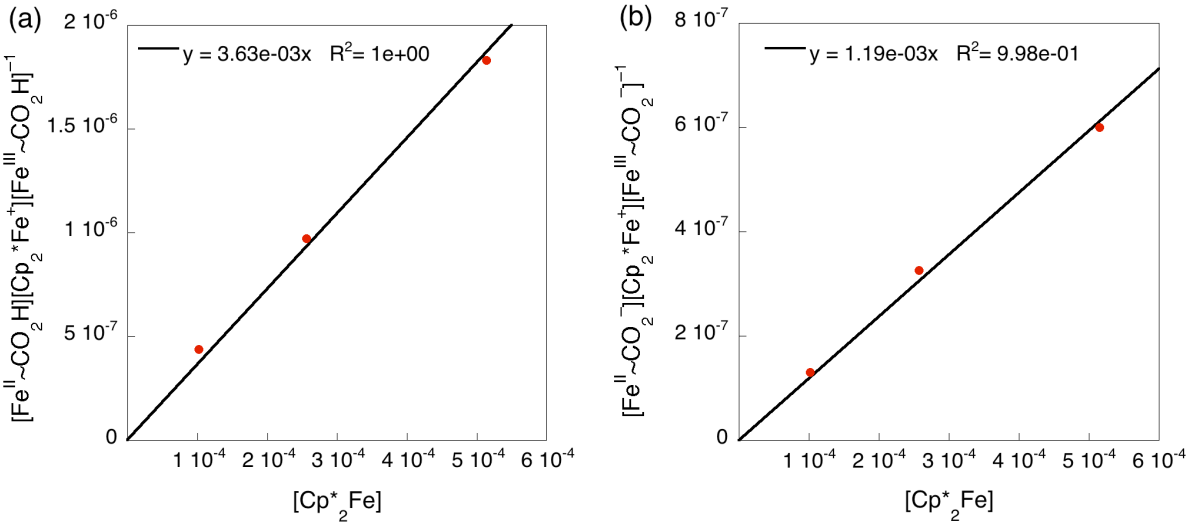

Figure S5. Mass balance plot for the titration of (a) $\mathbf{Fe^{III}\sim CO_2H}$ with Cp^*_2Fe and (b) $\mathbf{Fe^{III}\sim CO_2^-}$ with Cp^*_2Fe. The slope(s) give K_{eq} for each reaction, respectively.

(5) Gennett, T.; Milner, D. F.; Weaver, M. J.; *J. Phys. Chem.* **1985**, *89*, 2787-2794.

3.4 Stopped-flow kinetics for Fe^{III}~CO_2^- + *i*AscH$^-$ (eq 2)

Fe^{III}~CO_2^- (MeCN/0.1 ^{n}Bu$_4$NPF$_6$/5 mM MeIm) was freshly generated from **Fe^{III}~CO_2H** and 1 equivalent of DBU. k_2 was measured using 10-45 equivalents of *i*AscH$^-$. The kinetic data were analyzed using a first order model (Figure S6). Production of the ascorbyl radical product of reaction 2 was confirmed by EPR (Figure S7).

The rate constants for deuterium transfer were obtained in the same manner, with *i*AscD$^-$ from *i*AscD$_2$ + DBU. This measurement is complicated by the likely loss of the deuterium label by adventitious water in the MeCN. By Karl-Fischer titration the minimum water content is 6×10^{-4} M, roughly the same concentration as *i*AscD$^-$ used in this study. At the higher concentrations of *i*AscD$^-$ the isotope effect becomes slightly more pronounced, consistent with wash-out of the deuterium label. The ratio of pseudo-first-order rate constants yields $k_H/k_D = 1.2 \pm 0.1$, which should be taken as the *minimum* KIE. Attempts to add millimolar quantities of D_2O to these reaction mixtures (to ensure deuterium enrichment) results in anomalous kinetic behavior, which is probably because the thermodynamics and kinetics of ascorbate reactions are sensitive to the presence of hydrogen bond donors.[Error! Bookmark not defined.b]

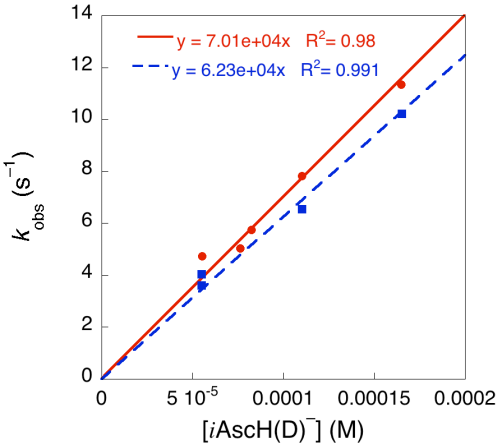

Figure S6. Pseudo-first-order plots for the reaction of *i*AscH$^-$ + **Fe^{III}~CO_2^-** (red, solid line) and *i*AscD$^-$ + **Fe^{III}~CO_2^-** (blue, dashed line). The second order rate constants $k_{1,H}$ and $k_{1,D}$ are given by the slopes of the lines.

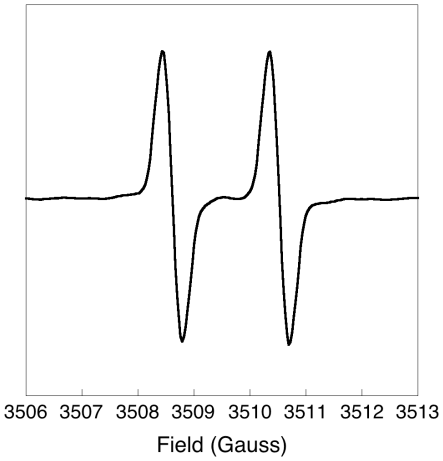

Figure S7. EPR spectrum of *i*Asc$^{\bullet-}$ from $\mathbf{Fe^{III}{\sim}CO_2^-}$ + *i*AscH$^-$ (reaction 2, main text). The hyperfine coupling constant is 1.91 G, in excellent agreement with a previous report.**Error! Bookmark not defined.**[a]

3.5 Stopped-flow kinetics for $\mathbf{Fe^{III}{\sim}CO_2H}$ + *i*AscH$^-$

Kinetics were performed as above, but using $\mathbf{Fe^{III}{\sim}CO_2H}$ or $Fe^{III}PPIX_{DME}(MeIm)_2OTf$. These reactions proceeded to partial completion based on the known spectra of the ferrous complexes. A comparison of data for $\mathbf{Fe^{III}{\sim}CO_2H}$ + *i*AscH$^-$ and $\mathbf{Fe^{III}{\sim}CO_2^-}$ + *i*AscH$^-$ under identical conditions is shown in Figure S8. The data for $Fe^{III}PPIX_{DME}(MeIm)_2OTf$ + *i*AscH$^-$ are essentially identical. The data in Figure S8 are well described by a second-order kinetic model with $k = 2.5 \pm 0.5 \times 10^4$ M^{-1} s^{-1}. Using the known spectrum of $\mathbf{Fe^{II}{\sim}CO_2H}$ as a reference gives $K = 0.13 \pm 0.04$ for this reaction.

The electron transfer reaction from *i*AscH$^-$ to $\mathbf{Fe^{III}{\sim}CO_2H}$ is 6 kcal mol^{-1} ($K_{ET} = 4 \times 10^{-5}$) uphill, inconsistent with the above equilibrium constant. However, the added 5 mM MeIm (pK_a = 12.2 in MeCN[6]) could accept a proton from *i*AscH$^{\bullet}$ (pK_a = 14) that would be generated from initial ET to $\mathbf{Fe^{III}{\sim}CO_2H}$, in effect driving the reaction more to completion. This could be why this "ET" reaction proceeds to ~70-80% completion under conditions identical to the PCET reactions discussed above. Indeed, adding varying amounts of MeIm (1-20 mM) to reactions of $Fe^{III}PPIX_{DME}(MeIm)_2OTf$ + *i*AscH$^-$ pushes the reaction more towards completion (with

(6) Kozak, A.; Czaja, M.; Chmurzyński, L. *J. Chem. Thermodynamics* **2006**, *38*, 599-605.

increasing [MeIm]) based upon absorbance changes. Reactions of $\mathbf{Fe^{III}{\sim}CO_2^-}$ + *i*AscH$^-$ do not show this imidazole dependence between 5 and 20 mM MeIm, which indicates that the propionate is acting as the proton acceptor in these cases. In any case, under identical conditions, reaction of $\mathbf{Fe^{III}{\sim}CO_2H}$ + *i*AscH$^-$ is slower than reaction of $\mathbf{Fe^{III}{\sim}CO_2^-}$ + *i*AscH$^-$. This is inconsistent with $\mathbf{Fe^{III}{\sim}CO_2^-}$ + *i*AscH$^-$ proceeding by initial ET since the former reaction is more favorable. The above data also indicate that the propionate accepts the ascorbate proton upon oxidation, not the MeIm that is also in solution.

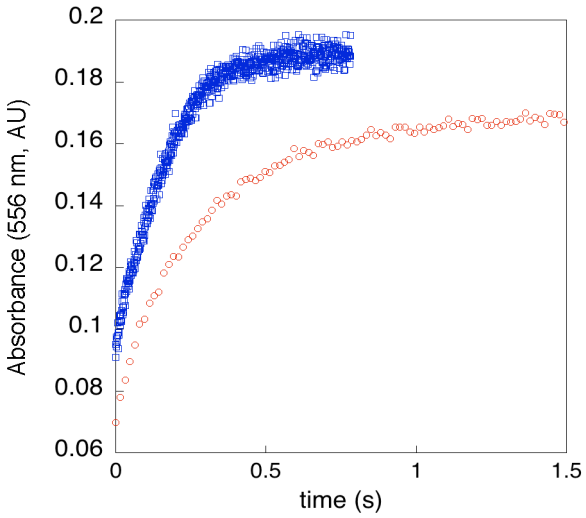

Figure S8. Kinetic traces for reaction of $\mathbf{Fe^{III}{\sim}CO_2^-}$ (1.0×10^{-5} M) with *i*AscH$^-$ (4.0×10^{-5} M) (blue □) and the reaction of $\mathbf{Fe^{III}{\sim}CO_2H}$ (1.0×10^{-5} M) with *i*AscH$^-$ (4.0×10^{-5} M) (red ○).

3.6 Stopped-flow reactions for $Fe^{III/II}$~CO_2(H) with quinone, hydroquinone and $^tBu_3PhO^\bullet$

Stopped-flow kinetics for reaction S1 in both the forward and reverse directions were performed under pseudo-first-order conditions of excess hydroquinone or benzoquinone, respectively. The reactions proceed rapidly (>10 seconds) to equilibrium. Production of benzoquinone and hydroquinone were confirmed by ^{1}H NMR. Typical spectral changes for both reaction S1 and reaction –S1 are shown in Figure S9, and equilibrium constants were determined from these spectral changes.

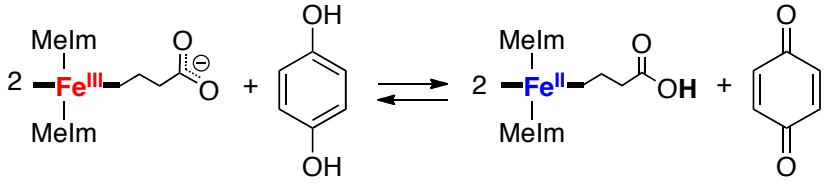

(S1)

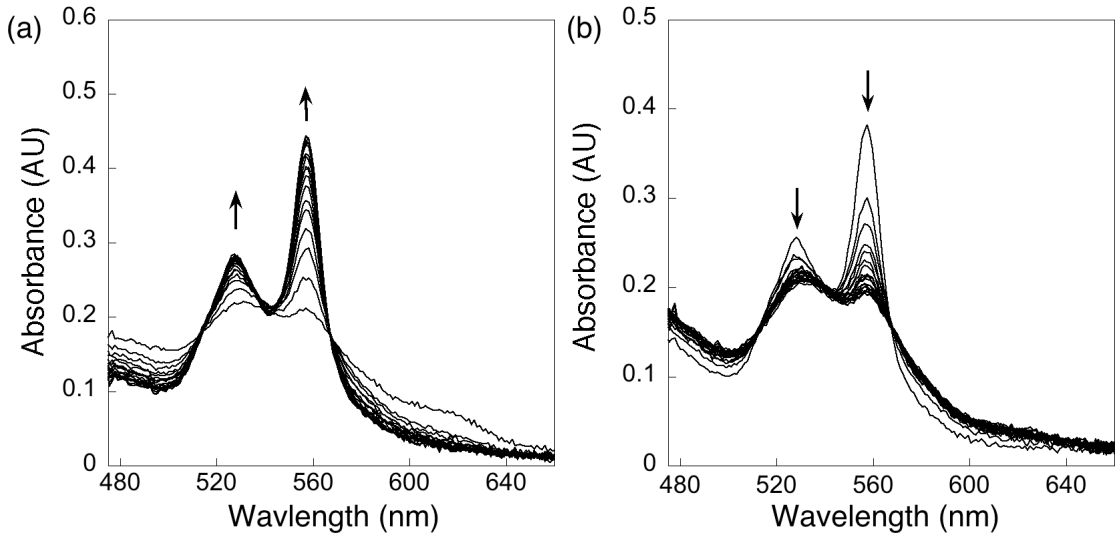

Figure S9. Kinetic data for the reaction of (a) $\mathbf{Fe^{III}}$~$\mathbf{CO_2^-}$ (23 μM) + 575 μM hydroquinone in MeCN, and (b) $\mathbf{Fe^{III}}$~$\mathbf{CO_2^-}$ (23 μM) + 575 μM benzoquinone in MeCN.

Stopped flow kinetics for $\mathbf{Fe^{II}}$~$\mathbf{CO_2H}$ + $^tBu_3PhO^\bullet$ were performed at the lowest practical concentrations. The reaction of 1.5×10^{-5} M $\mathbf{Fe^{II}}$~$\mathbf{CO_2H}$ with 1.5×10^{-5} M $^tBu_3PhO^\bullet$ is complete within the mixing time of the stopped flow spectrophotometer. This indicates $t_{1/2} < 3$ ms which implies a second order rate constant $\geq 10^7$ M^{-1} s^{-1}. This result is the same as for the analogous reaction of (tetraphenylporphyrin)Fe^{II}(4-MeImH)$_2$ with $^tBu_3PhO^\bullet$.[7]

(7) Warren, J. J.; Mayer, J. M. *J. Am. Chem. Soc.* **2008**, *131*, 2774-2776.

4. TEMPO(H) UV-Vis kinetics

In an inert atmosphere glove box, 3 mL aliquots of a 2.5 × 10^{-5} M stock solution of **Fe^{III}~CO_2H** were placed in quartz cuvettes and capped with a screw top lid and Teflon™ coated septa. A new septum was used for each kinetic run. Kinetics were performed under an atmosphere of flowing nitrogen on an HP 8453 diode array using a Unisoku Unispeks thermostated cuvette holder at 25°C. A DBU solution (prepared in the glovebox, 25 µL of a 2.4 mM solution; 1 equiv) was injected into the cuvette to generate **Fe^{III}~CO_2^-**, then an aliquot (10-100 eq) of a concentrated TEMPOH solution (2.4 mM) was injected into each cuvette. Spectra were collected automatically every 5 seconds, incrementing to longer intervals at long times. Runs were stopped when the reactions were judged complete based on the observed spectral changes. The production of TEMPO was confirmed by EPR (Figure S14). Kinetic data were analyzed using SPECFIT™ software with a first-order kinetic model. Plots of the observed first order rate constants as a concentration of TEMPO(H) are shown in Figures S10 and S12.

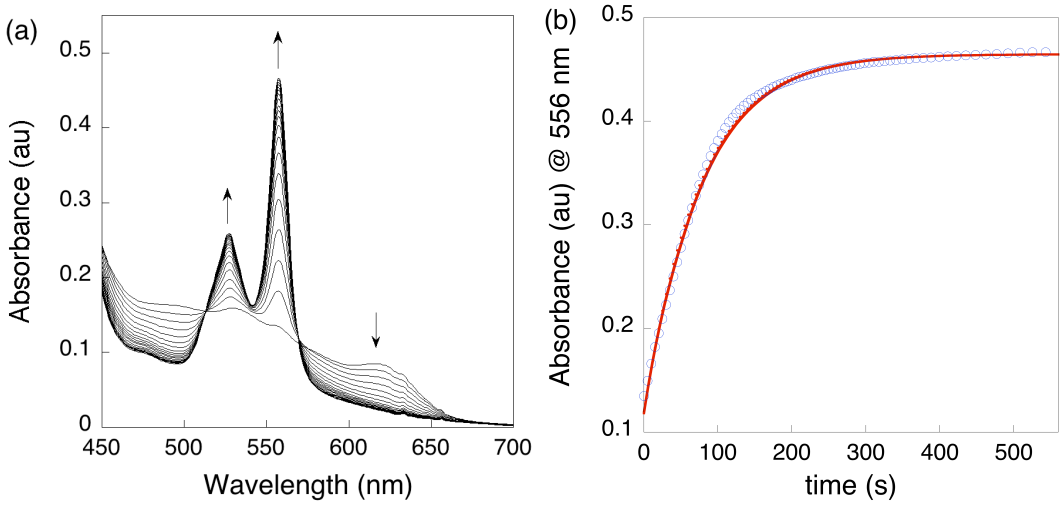

Figure S10. Kinetic data for the reaction of **Fe^{III}~CO_2^-** (20.3 µM) + 1.06 mM TEMPOH in MeCN: (a) overlay plot showing selected spectra and (b) trace of the kinetic data at 556 nm (○) with the first-order fit of the data (—).

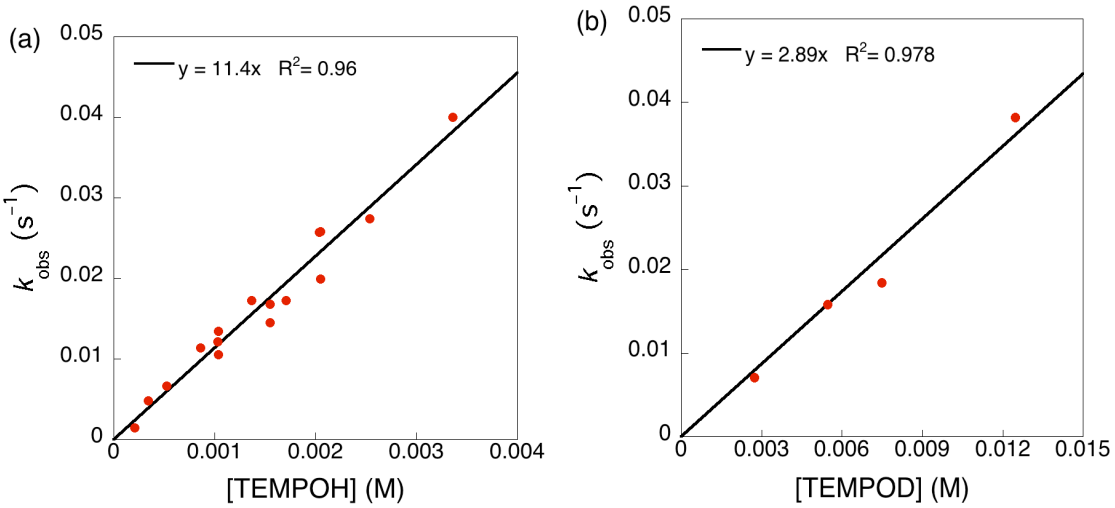

Figure S11. Pseudo-first-order plots for the reaction of (a) TEMPOH + $\mathbf{Fe^{III}}$**~CO₂⁻** and (b) TEMPOD + $\mathbf{Fe^{III}}$**~CO₂⁻**. The second order rate constants $k_{4,H}$ and $k_{4,D}$ are given by the slopes of the lines.

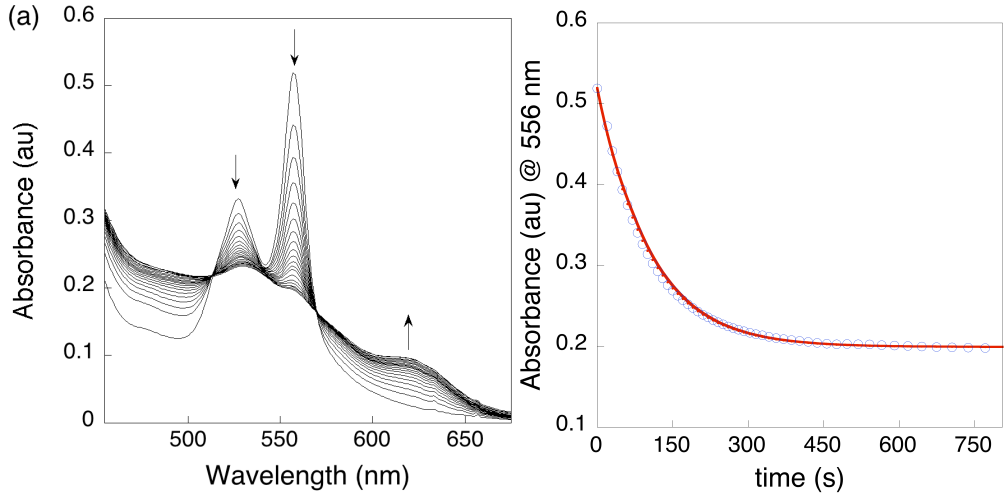

Figure S12. Kinetic data for the reaction of $\mathbf{Fe^{II}}$**~CO₂H** (27.6 μM) + 2.48 mM TEMPO• in MeCN: (a) overlay plot showing selected spectra and (b) trace of the kinetic data at 556 nm (○) with the first-order fit of the data (—).

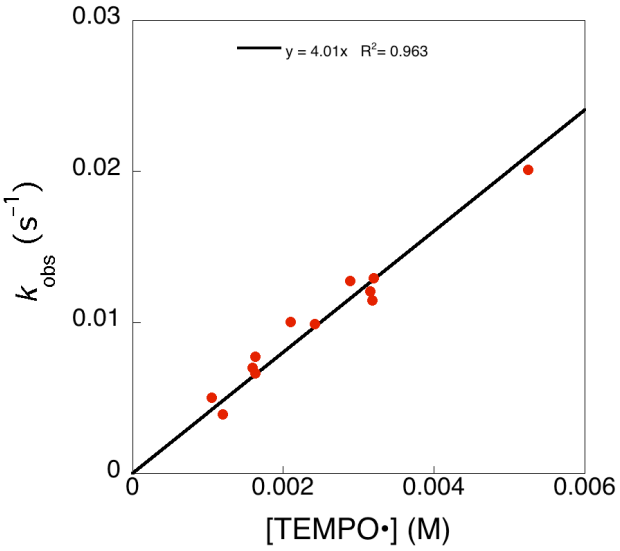

Figure S13. Pseudo-first-order plot for the reaction of TEMPO$^{\bullet}$ + **Fe^{II}~CO$_2$H**. The second order rate constant k_{-2} is given by the slope of the line.

Figure S14. EPR spectrum of TEMPO from **Fe^{III}~CO$_2^-$** + TEMPOH (reaction 4, main text). The hyperfine coupling constant is 15.8 G, in excellent agreement with a previous report.[8]

(8) Mori, H.; Ohara, M.; Kwan, T. *Chem. Pharm. Bull.* **1980**, *28*, 3178-3183.